ISBN: 978-3-95450-230-1 ISSN: 2673-5350 doi:10.18429/JACoW-IBIC2021-TUOA04

MEASUREMENT AND RECONSTRUCTION OF A BEAM PROFILE USING A GAS SHEET MONITOR BY BEAM-INDUCED FLUORESCENCE DETECTION IN J-PARC

Ippei Yamada*[1], Motoi Wada
Graduate School of Science and Engineering, Doshisha University, Kyoto, Japan
Katsuhiro Moriya, Junichiro Kamiya, Michikazu Kinsho
Japan Atomic Energy Agency, J-PARC center, Ibaraki, Japan
[1]also at Japan Atomic Energy Agency, J-PARC center

Abstract

A non-destructive transverse beam profile monitor using interaction between a beam and a gas sheet has been developed and demonstrated in J-PARC. The gas sheet formed based on rarefied gas dynamics enables two-dimensional beam profile measurement by detection of induced fluorescence as a 2D image with a CCD camera. The relative-sensitivity spatial distribution of the developed monitor was measured to quantitatively reconstruct a beam profile from the captured image. The sensitivity distribution consists of the sheet-gas density spatial distribution, non-uniformity of the incident solid angle, and the detection efficiency distribution of the CCD camera. The J-PARC 3 MeV H^- beam profile was successfully reconstructed with deviation of 7% ± 2% by the integral equation derived from the monitor's principle with the sensitivity distribution.

INTRODUCTION

A non-destructive or a minimal destructive diagnostic system, which is advantageous for constant monitoring, plays an important role for high-intensity, high-energy beam accelerator operation. The system enables to minimize beam losses and radioactivations of the accelerator components. We have developed a non-destructive transverse beam profile monitor, *the gas sheet monitor*, using interaction between a beam and an injected sheet-shaped gas [1]. The gas sheet is formed based on a technique of rarefied gas dynamics to increase a local gas density. The sheet gas interacts with a high intensity beam and induces photons whose spatial distribution depends on the gas density spatial distribution and the beam intensity spatial distribution in transverse. The two-dimensional beam profile can be obtained by taking a picture of the fluorescence and applying a proper analysis considering the effect of the gas density distribution. Figure 1 shows the development flow of the gas sheet monitor. Development of the gas sheet monitor is separated into four components: (1) formation of gas sheet, (2) evaluation of the gas density spatial distribution, (3) test of the profile measurement using a high intensity beam, and (4) reconstruction of the beam profile. In this paper, we report the details of the beam profile measurement with the gas sheet monitor from the four viewpoints.

* ip_yamada@icloud.com

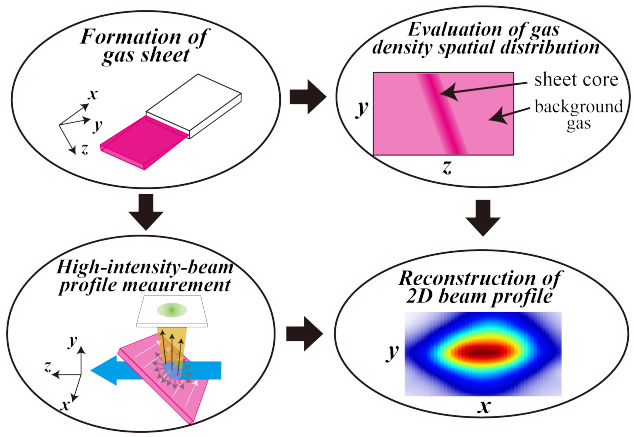

Figure 1: A development flow of the gas sheet beam profile monitor system.

PRINCIPLE

Gas Sheet Formation

The gas sheet is formed based on rarefied gas dynamics. When the mean free path of gas molecules is longer than the typical vacuum chamber dimension like in a beam pipe, the motion of gas molecules is determined not by intermolecular collisions but by the thermal motion and reflections with the chamber wall. The incident angle for reflections with a wall does not affect the reflection angle, and the probability distribution function of the reflection angle θ with respect to the normal direction of the wall is proportional to $\cos\theta$: cosine law. A long gas conduit of a thin cross section can form a gas sheet by increasing the number of reflections in the thickness direction for molecules to obtain a large angle. In this condition, the motion of gas molecules can be modeled by the individual motion of the constant velocity with reflections being subject to the cosine law, such as Molflow+ code [2].

Beam Profile Measurement

Figure 2 shows the gas sheet monitor consisting of a gas sheet flowing along x axis and a photon detector integrating fluorescence induced by beam-gas interaction along y axis. The high intensity beam passes through the gas sheet along z axis. The photons are induced by interaction between the beam and not only the gas sheet but also the background gas.

ISBN: 978-3-95450-230-1 ISSN: 2673-5350 doi:10.18429/JACoW-IBIC2021-TUOA04

The detected luminous intensity spatial distribution $g(x,z)$ is constructed by the produced photon spatial distribution, the detection efficiency spatial distribution of the image sensor array, and non-uniformity of the solid angle. The latter two effects are integrated as the detection efficiency spatial distribution of the gas sheet monitor, $\alpha(x,y,z)$. The relation among the detected luminous intensity spatial distribution $g(x,z)$, the transverse beam profile $F(x,y)$, the gas density spatial distribution $n(x,y,z)$, and the detection efficiency spatial distribution $\alpha(x,y,z)$ can be written as an integral equation,

$$g(x,z) = \int_D \alpha(x,y,z) \cdot n(x,y,z) \cdot F(x,y)\mathrm{d}y \quad (1)$$

$$\equiv \int_D k(x,y,z) \cdot F(x,y)\mathrm{d}y \quad (2)$$

where D is the integral region larger than the full beam width in y direction, such as a beam pipe. The distribution $k(x,y,z)$ is defined as the relative-sensitivity spatial distribution of the gas sheet monitor. The beam profile $F(x,y)$ can be reconstructed from the obtained luminous intensity distribution $g(x,z)$ by giving the relative-sensitivity distribution $k(x,y,z)$ and solving Eq. (2).

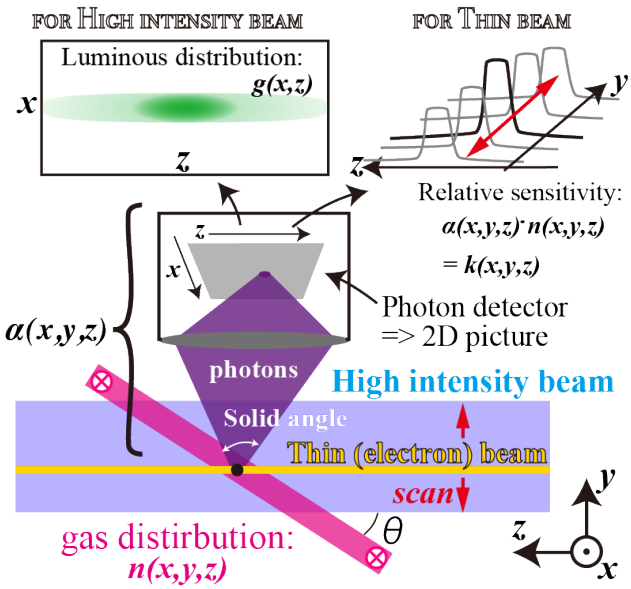

Figure 2: The principle of the gas sheet monitor.

The relative-sensitivity spatial distribution can be measured by injecting a thin beam into the gas sheet monitor. The center position of the thin beam, the beam widths, and the beam profile are defined as (x_0, y_0), Δx, Δy, and $F_{\mathrm{thin}}(x,y)$, respectively. A thin beam induces photons in a limited local volume,

$$g(x,z) = \int_{\Delta y} k(x,y,z) \cdot F_{\mathrm{thin}}(x,y)\mathrm{d}y. \quad (3)$$

The measurement spatial resolutions are regarded as the thin beam widths Δx and Δy, and the luminous signal is integrated along x axis,

$$\int_{\Delta x} g(x,z)\mathrm{d}x = \int_{\Delta x}\int_{\Delta y} k(x,y,z) \cdot F_{\mathrm{thin}}(x,y)\mathrm{d}x\mathrm{d}y \quad (4)$$

$$G(z) = \tilde{F}_{\mathrm{thin}} \cdot k(x_0, y_0, z) \quad (5)$$

where $\tilde{F}_{\mathrm{thin}}$ is the luminous intensity coefficient for thin beam injection. The obtained distribution $G(z)$ is in proportion to the one-dimensional sensitivity spatial distribution. Scanning the thin beam position (x_0, y_0) gives the three-dimensional relative-sensitivity distribution, if the coefficient $\tilde{F}_{\mathrm{thin}}$ is constant over the scanned area.

DEVELOPED GAS SHEET MONITOR

The developed gas sheet monitor system consisting of a gas sheet generator, a cover chamber with a slit, a main chamber attached to a beam line, and a photon detector system is shown in Fig 3. The gas sheet generator is a cuboid conduit of 100 mm × 50 mm × 0.1 mm. A cover chamber having a rectangular slit of 50 mm × 0.5 mm with a turbomolecular pump which has a 420 ℓ/s pumping speed for N_2 surrounds the gas sheet generator to cut the gas-sheet distribution tail. Figure 4 shows the calculated gas flux spatial distribution along the thickness direction at the beam-gas interaction point for N_2 gas. The gas sheet with 0.5 mm thickness for full width at half maximum can be formed by the conduit, and the cover chamber with 420 ℓ/s pumping reduces the tali part intensity. The N_2 gas sheet entering the main chamber through the slit interacts with the beam and is evacuated by a turbomolecular pump and a cryo pump with the pumping speeds of 300 ℓ/s and 750 ℓ/s for N_2, respectively. The photon detector system consists of a set of optical lenses, an image intensifier, and a CCD camera. The diameter of the optical lenses is 50 mm and the distance from the beam-gas interaction point to the objective lens is 200 mm. The image intensifier increases the signal intensity up to 10^4 times. The CCD camera has 1920 × 1080 sensors of 16 bit.

RELATIVE-SENSITIVITY DISTRIBUTION

The relative-sensitivity spatial distribution was measured with a 3 keV, 10 μA, DC electron beam as a thin beam in Fig. 2. An example of the image captured by the sensitivity spatial distribution measurement is shown in Fig. 5. The total exposure time was 20 minutes (=120 s × 10 frames). The inlet pressure of the sheet generator was 100 Pa and the pressure of the main chamber was 5.7 × 10^{-5} Pa. The white part describes the photon signal produced by beam-gas interaction. The one-dimensional sensitivity distribution $k(x_0, y_0, z)$ can be constructed by integrating the luminous intensity along x axis in 1 mm. The two-dimensional relative-sensitivity distribution $k(x_0, y, z)$ constructed by scanning the electron beam position along y axis is shown in Fig. 6.

MEASUREMENT AND RECONSTRUCTION OF BEAM PROFILE

The high-intensity-beam profile was measured using the J-PARC 3 MeV, 60 mA H^- beam at the MEBT test stand [1, 3].

ISBN: 978-3-95450-230-1 ISSN: 2673-5350 doi:10.18429/JACoW-IBIC2021-TUOA04

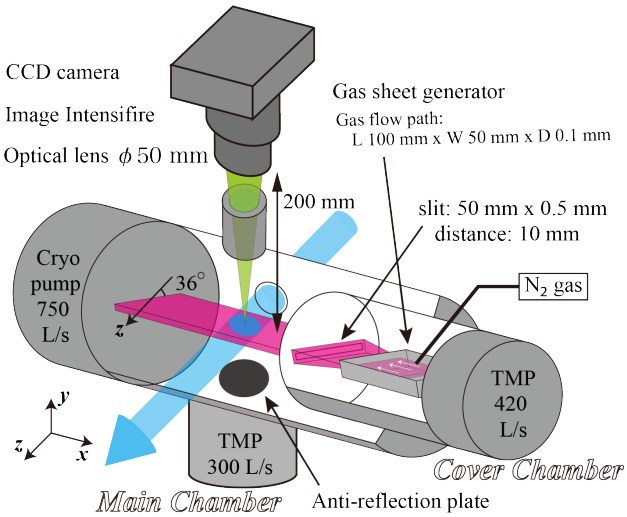

Figure 3: The developed gas sheet monitor system. The monitor system dimensions are 1,500 mm × 600 mm × 220 mm in x, y and z direction, respectively.

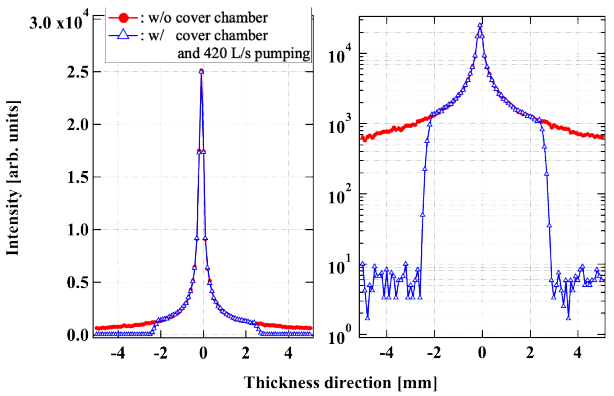

(a) linear plots (b) semi-log plots

Figure 4: The simulated gas flux spatial distribution along the sheet thickness direction at the beam-gas interaction point.

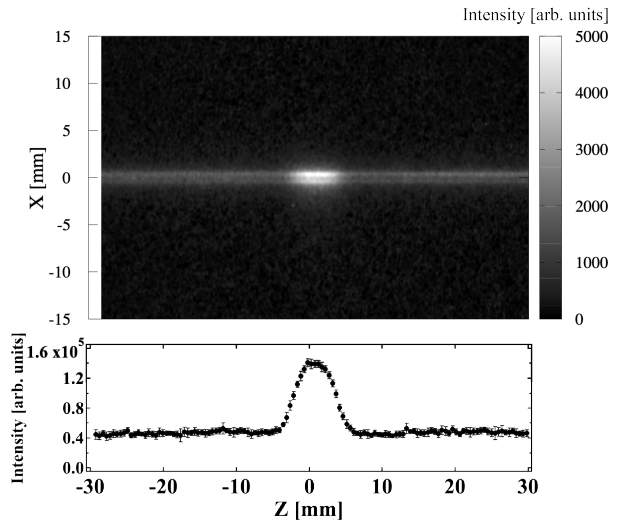

Figure 5: An example of the captured image of the photons produced by beam-gas interaction and the one-dimensional sensitivity distribution $k(x_0, y_0, z)$ constructed by integrating the luminous intensity along x direction.

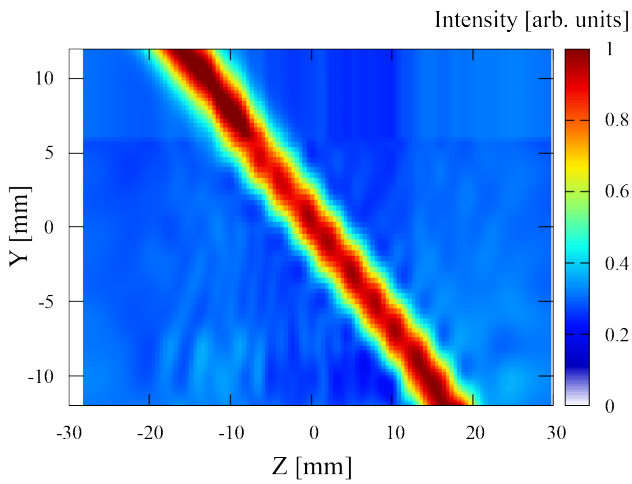

Figure 6: The two-dimensional relative-sensitivity spatial distribution in y-z plane: $k(x_0, y, z)$.

An example of the captured image is shown in Fig. 7. The image was captured using 1.7×10^{15} H^- particles/frame and was averaged over 80 frames. The inlet pressure of the sheet generator was 100 Pa and the pressure of the main chamber was 5.6×10^{-5} Pa. The image describes that the photon signals produced not only by the gas sheet core but also by the background gas are detected. The beam profile should be reconstructed from the image and the measured relative-sensitivity distribution with Eq. (2). Solving the integral equation numerically is not easy because the numerical method needs over 100-order-digit precision. Regarding the integral equation as an integral formula, the function $g_{\mathrm{int}}(x, z)$ is defined as an integral of the measured sensitivity distribution and an assumed beam profile. The distribution $g_{\mathrm{int}}(x, z)$ is compared with the distribution $g_{\mathrm{H^-}}(x, z)$ which is the image shown in Fig. 7 obtained by beam profile measurement. When these two distributions $g_{\mathrm{int}}(x, z)$ and $g_{\mathrm{H^-}}(x, z)$ agree each other, the assumed beam profile is considered to be the actual beam profile.

The beam profile is approximated with a set of 21 parameters $a = (a_0, a_1, \cdots, a_{10}), b = (b_1, b_2, \cdots, b_{10})$,

$$F(x_0, y; a, b) = \frac{a_0}{2} + \sum_{k=1}^{10} \left\{ a_k \cos\left(k\frac{\pi y}{L}\right) + b_k \sin\left(k\frac{\pi y}{L}\right) \right\} \quad (6)$$

where L is the half length of the beam-defined region. The beam profile assumed by Eq. (6) is optimized using the Nelder-Mead method [4]. The method optimizes the N parameters not by calculating the derivative of the objective function but by geometrically moving the parameters to minimize a simplex constructed from vertices of the objective function for $N + 1$ sets of the parameters. The objective func-

ISBN: 978-3-95450-230-1 ISSN: 2673-5350 doi:10.18429/JACoW-IBIC2021-TUOA04

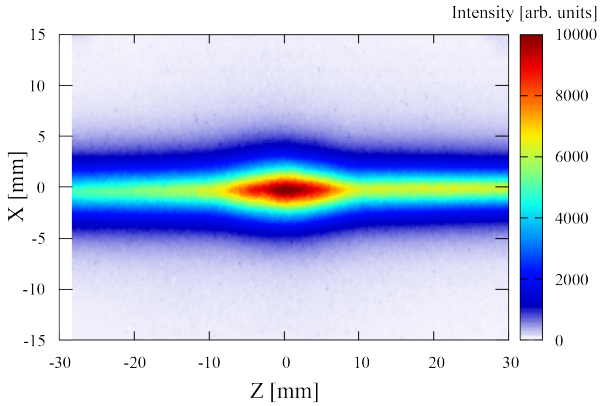

Figure 7: The image obtained by the high-intensity-beam profile measurement. This two-dimensional luminous intensity distribution is defined as $g_{H^-}(x,z)$.

tion is defined as a deviation between $g_{\mathrm{int}}(x,z)$ and $g_{H^-}(x,z)$:

$$s(a,b,x_0) = \sqrt{\frac{1}{M}\sum_{i=1}^{M}\left\{\frac{g_{H^-}(x_0,z_i) - g_{\mathrm{int}}(x_0,z_i;a,b)}{g_{H^-}(x_0,z_i)}\right\}^2}. \quad (7)$$

The 22 initial beam profiles are defined with Fourier series of Gaussian distributions whose σ are 2-4 mm. The reiteration of the optimization is terminated when the normalized simplex volume becomes smaller than some limit:

$$\frac{s_{\max} - s_{\min}}{\frac{1}{N+1}\sum_{i=1}^{N+1} s(a_i,b_i)} < T_h. \quad (8)$$

Figure 8 shows the result of the beam profile optimization with $T_h = 0.001$ at $x_0 = 3.0$ mm. The distributions $g_{H^-}(x_0,z)$ and $g_{\mathrm{int}}(x_0,z)$ agree each other with the deviation defined as Eq. (7) of 3% ± 1%. The reconstructed (optimized) profile $F(x_0,y)$ is also shown in Fig. 8. Reconstructing the beam profiles $F(x_0,y)$ for each x and arraying the profiles for x direction yield the two-dimensional beam profile shown in Fig. 9 with the deviation of 7% ± 2% on average.

CONCLUSION

We demonstrated that the relative-sensitivity spatial distribution can be measured by injecting the thin electron beam into the gas sheet monitor and the high-intensity-beam profile can be quantitatively reconstructed using the devised integral equation with the measured sensitivity distribution. The proposed method from constructing a relative-sensitivity distribution to reconstructing a high-intensity-beam profile can be applied to any profile monitor based on beam-gas interaction. We are starting to use the gas sheet monitor for investigating time development of the beam profile in a beam pulse and investigating an effect of gas injection on the beam quality.

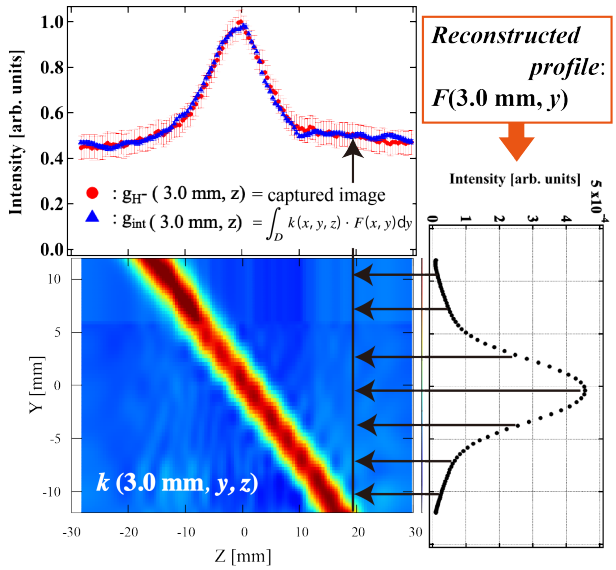

Figure 8: Reconstruction of the beam profile by comparing the distributions $g_{H^-}(x_0,z)$ and $g_{\mathrm{int}}(x_0,z)$ which is calculated by Eq. (2) with the relative-sensitivity distribution $k(x_0,y,z)$ and the assumed beam profile $F(x_0,y)$. The error bars describe the standard deviation of the measurement.

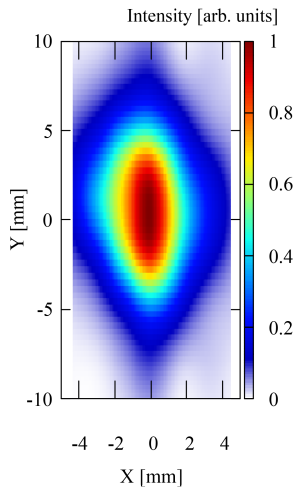

Figure 9: The reconstructed two-dimensional beam profile of the J-PARC 3MeV H^- beam.

REFERENCES

[1] I. Yamada *et al.*, "High-intensity beam profile measurement using a gas sheet monitor by beam induced fluorescence detection", *Phys. Rev. Accel. Beams*, vol. 24, p. 042801, 2021.

[2] Molflow+, `http://molflow.we.cern.ch`

[3] Y. Kondo *et al.*, "Upgrade of the 3-MeV Linac for testing of Accelerator Components at J-PARC", *Journal of Physics: Conference Series*, vol. 1350, p. 012077, 2019.

[4] J. A. Nelder and R. Mead, "A simplex method for function minimization", *The Computer Journal*, vol. 7, p. 308313, 1965.